

Online Journal of Space Communication

Volume 2
Issue 3 *Remote Sensing of Earth via Satellite*
(Winter 2003)

Article 8

January 2003

Introduction to Hyperspectral Image Analysis

Peg Shippert

Follow this and additional works at: <https://ohioopen.library.ohio.edu/spacejournal>



Part of the [Astrodynamics Commons](#), [Navigation, Guidance, Control and Dynamics Commons](#), [Space Vehicles Commons](#), [Systems and Communications Commons](#), and the [Systems Engineering and Multidisciplinary Design Optimization Commons](#)

Recommended Citation

Shippert, Peg (2003) "Introduction to Hyperspectral Image Analysis," *Online Journal of Space Communication*: Vol. 2 : Iss. 3 , Article 8.

Available at: <https://ohioopen.library.ohio.edu/spacejournal/vol2/iss3/8>

This Research Reports is brought to you for free and open access by the OHIO Open Library Journals at OHIO Open Library. It has been accepted for inclusion in Online Journal of Space Communication by an authorized editor of OHIO Open Library. For more information, please contact deborded@ohio.edu.

Introduction to Hyperspectral Image Analysis

Peg Shippert, Ph.D.
 Earth Science Applications Specialist
 Research Systems, Inc.

Background

The most significant recent breakthrough in remote sensing has been the development of hyperspectral sensors and software to analyze the resulting image data. Fifteen years ago only spectral remote sensing experts had access to hyperspectral images or software tools to take advantage of such images. Over the past decade hyperspectral image analysis has matured into one of the most powerful and fastest growing technologies in the field of remote sensing.

The “hyper” in hyperspectral means “over” as in “too many” and refers to the large number of measured wavelength bands. Hyperspectral images are spectrally overdetermined, which means that they provide ample spectral information to identify and distinguish spectrally unique materials. Hyperspectral imagery provides the potential for more accurate and detailed information extraction than possible with any other type of remotely sensed data.

This paper will review some relevant spectral concepts, discuss the definition of hyperspectral versus multispectral, review some recent applications of hyperspectral image analysis, and summarize image-processing techniques commonly applied to hyperspectral imagery.

Spectral Image Basics

To understand the advantages of hyperspectral imagery, it may help to first review some basic spectral remote sensing concepts. You may recall that each photon of light has a wavelength determined by its energy level. Light and other forms of electromagnetic radiation are commonly described in terms of their wavelengths. For example, visible light has wavelengths between 0.4 and 0.7 microns, while radio waves have wavelengths greater than about 30 cm (Fig. 1).

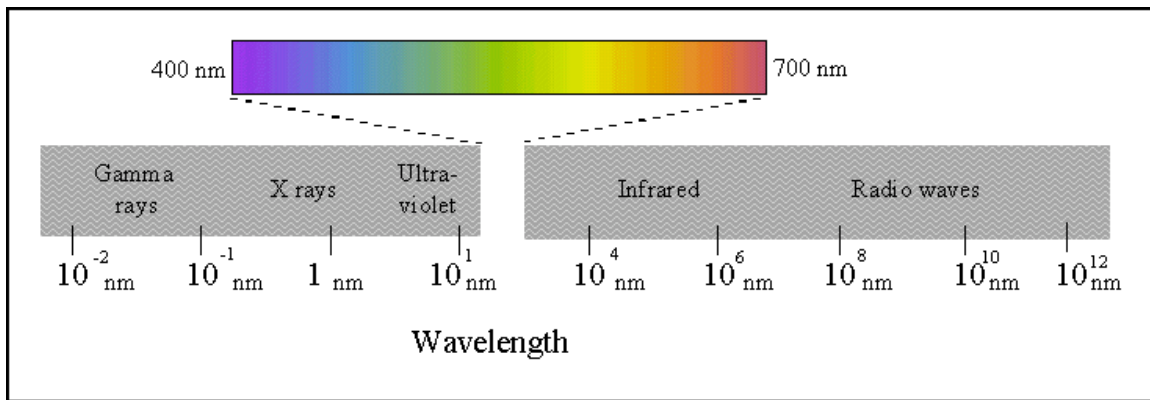


Figure 1. The electromagnetic spectrum

Reflectance is the percentage of the light hitting a material that is then reflected by that material (as opposed to being absorbed or transmitted). A reflectance spectrum shows the reflectance of a material measured across a range of wavelengths (Fig. 2). Some materials will reflect certain wavelengths of light, while other materials will absorb the same wavelengths. These patterns of reflectance and absorption across wavelengths can uniquely identify certain materials.

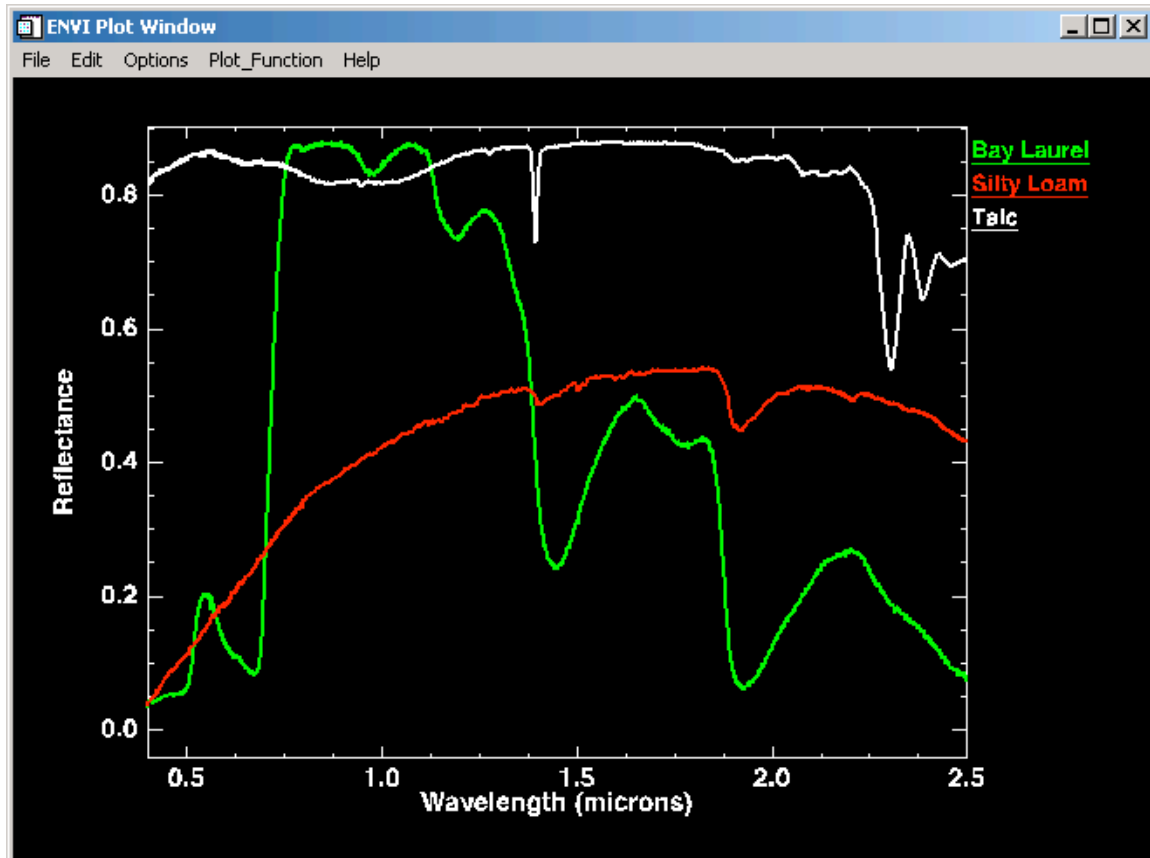


Figure 2. Reflectance spectra measured by laboratory spectrometers for three materials: a green bay laurel leaf, the mineral talc, and a silty loam soil.

Field and laboratory spectrometers usually measure reflectance at many narrow, closely spaced wavelength bands, so that the resulting spectra appear to be continuous curves (Fig. 2). When a spectrometer is used in an imaging sensor, the resulting images record a reflectance spectrum for each pixel in the image (Fig. 3).

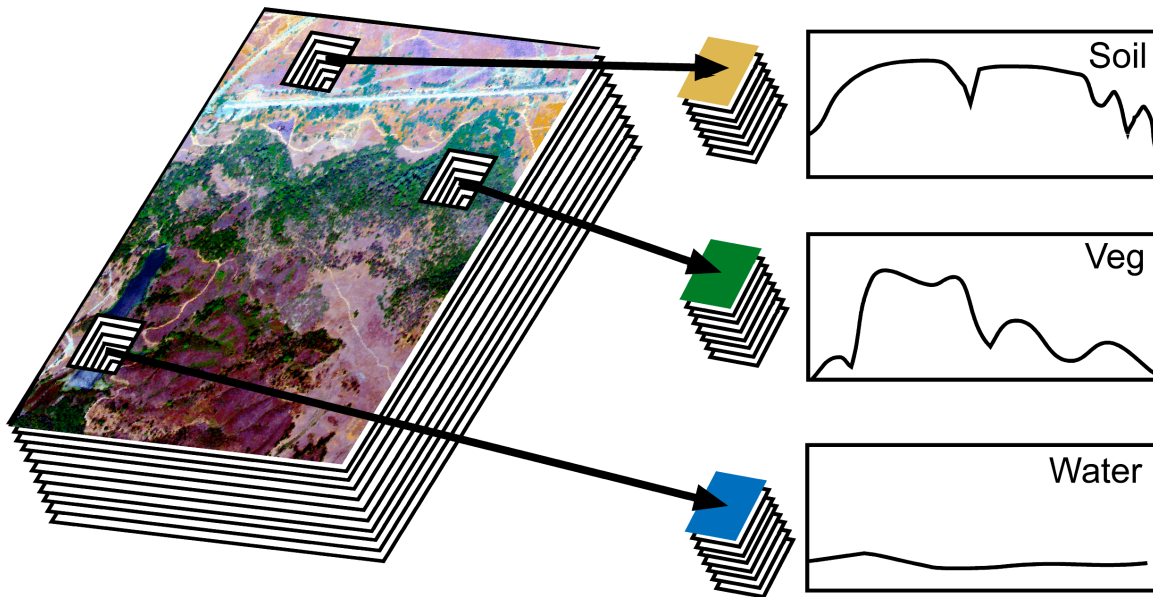


Figure 3. The concept of hyperspectral imagery. Image measurements are made at many narrow contiguous wavelength bands, resulting in a complete spectrum for each pixel.

Hyperspectral Data

Most multispectral imagers (e.g., Landsat, SPOT, AVHRR) measure radiation reflected from a surface at a few wide, separated wavelength bands (Fig. 4). Most hyperspectral imagers (Table 1), on the other hand, measure reflected radiation at a series of narrow and contiguous wavelength bands. When we look at a spectrum for one pixel in a hyperspectral image, it looks very much like a spectrum that would be measured in a spectroscopy laboratory (Fig. 5). This type of detailed pixel spectrum can provide much more information about the surface than a multispectral pixel spectrum.

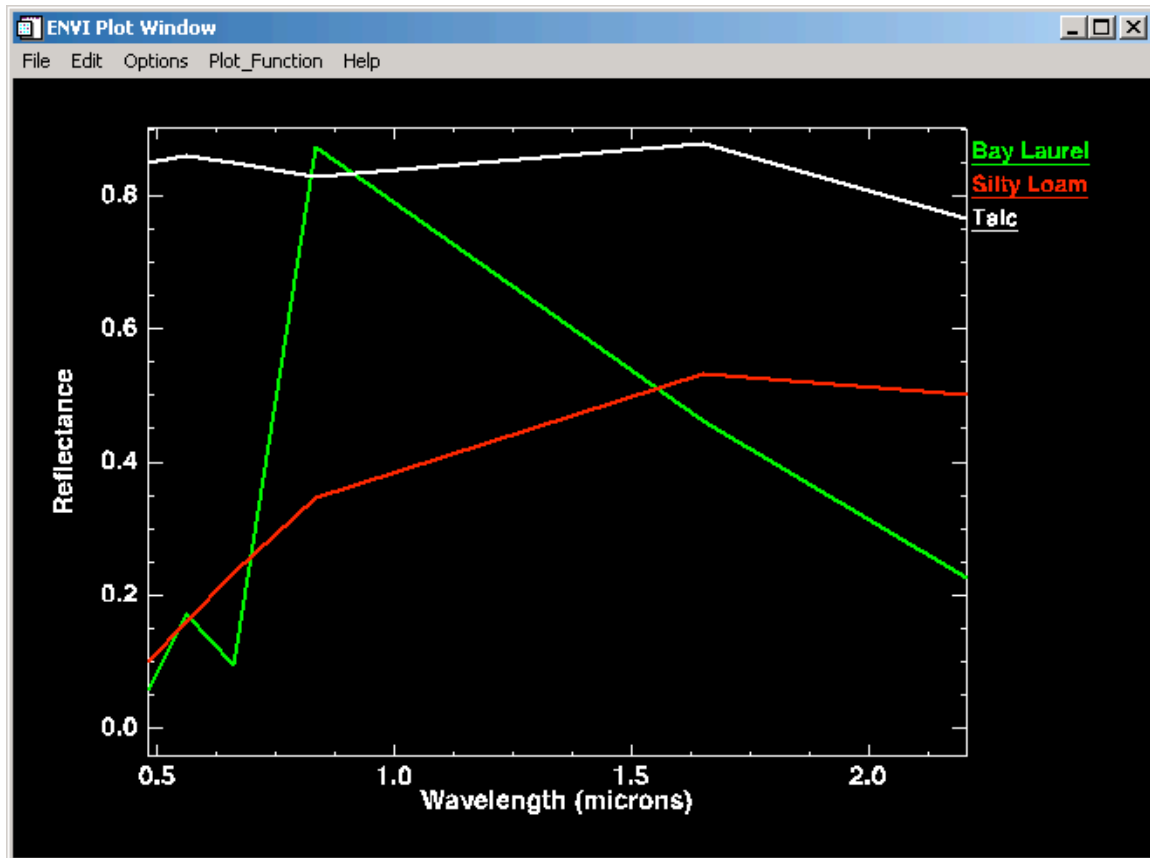


Figure 4. Reflectance spectra of the three materials in Figure 2 as they would appear to the multispectral Landsat 7 ETM sensor.

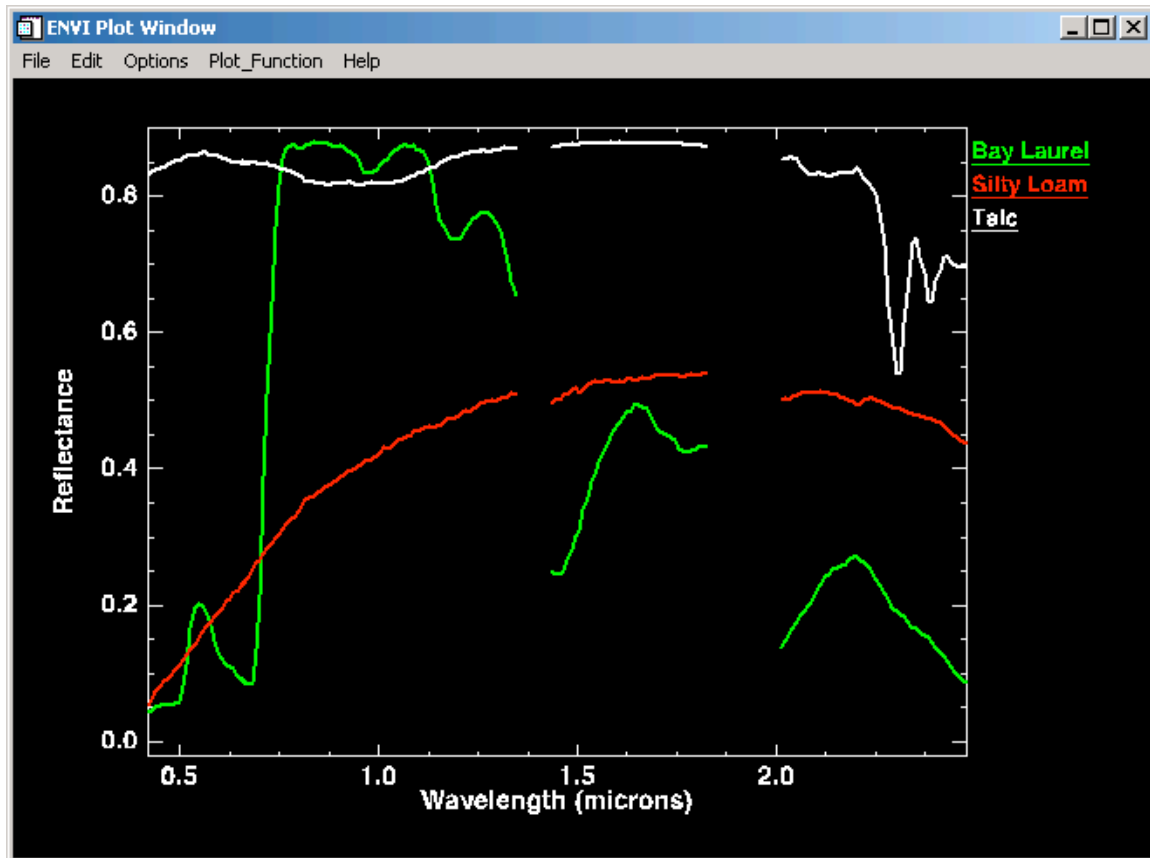


Figure 5. Reflectance spectra of the three materials in Figure 2 as they would appear to the hyperspectral AVIRIS sensor. The gaps in the spectra are wavelength ranges at which the atmosphere absorbs so much light that no reliable signal is received from the surface.

Although most hyperspectral sensors measure hundreds of wavelengths, it is not the number of measured wavelengths that defines a sensor as hyperspectral. Rather it is the narrowness and contiguous nature of the measurements. For example, a sensor that measured only 20 bands could be considered hyperspectral if those bands were contiguous and, say, 10 nm wide. If a sensor measured 20 wavelength bands that were, say, 100 nm wide, or that were separated by non-measured wavelength ranges, the sensor would no longer be considered hyperspectral.

Standard multispectral image classification techniques were generally developed to classify multispectral images into broad categories. Hyperspectral imagery provides an opportunity for more detailed image analysis. For example, using hyperspectral data, spectrally similar materials can be distinguished, and sub-pixel scale information can be extracted. To fulfill this potential, new image processing techniques have been developed.

Most past and current hyperspectral sensors have been airborne (Table 1), with two recent exceptions: NASA's Hyperion sensor on the EO-1 satellite, and the U.S. Air Force Research Lab's FTESI sensor on the MightySat II satellite. Several new space-based hyperspectral sensors have been proposed recently (Table 2). Unlike airborne

sensors, space-based sensors are able to provide near global coverage repeated at regular intervals. Therefore, the amount of hyperspectral imagery available should increase significantly in the near future as new satellite-based sensors are successfully launched.

Table 1. Current and Recent Hyperspectral Sensors and Data Providers

Satellite Sensors	Manufacturer	Number of Bands	Spectral Range
FTHSI on MightySat II	Air Force Research Lab www.vs.afrl.af.mil/TechProgs/MightySatII	256	0.35 to 1.05 μ m
Hyperion on EO-1	NASA Goddard Space Flight Center eol.gsfc.nasa.gov	220	0.4 to 2.5 μ m
Airborne Sensors	Manufacturer	Number of Bands	Spectral Range
AVIRIS (Airborne Visible Infrared Imaging Spectrometer)	NASA Jet Propulsion Lab makalu.jpl.nasa.gov/	224	0.4 to 2.5 μ m
HYDICE (Hyperspectral Digital Imagery Collection Experiment)	Naval Research Lab	210	0.4 to 2.5 μ m
PROBE-1	Earth Search Sciences Inc. www.earthsearch.com	128	0.4 to 2.5 μ m
casi (Compact Airborne Spectrographic Imager)	ITRES Research Limited www.itres.com	up to 228	0.4 to 1.0 μ m
HyMap	Integrated Spectronics www.intspec.com	100 to 200	Visible to thermal infrared
EPS-H (Environmental Protection System)	GER Corporation www.ger.com	VIS/NIR (76), SWIR1 (32), SWIR2 (32), TIR (12)	VIS/NIR (.43 to 1.05 μ m), SWIR1 (1.5 to 1.8 μ m), SWIR2 (2.0 to 2.5 μ m), and TIR

			(8 to 12.5 μm)
DAIS 7915 (Digital Airborne Imaging Spectrometer)	GER Corporation	VIS/NIR (32), SWIR1 (8), SWIR2 (32), MIR (1), TIR (6)	VIS/NIR (0.43 to 1.05 μm), SWIR1 (1.5 to 1.8 μm), SWIR2 (2.0 to 2.5 μm), MIR (3.0 to 5.0 μm), and TIR (8.7 to 12.3 μm)
DAIS 21115 (Digital Airborne Imaging Spectrometer)	GER Corporation	VIS/NIR (76), SWIR1 (64), SWIR2 (64), MIR (1), TIR (6)	VIS/NIR (0.40 to 1.0 μm), SWIR1 (1.0 to 1.8 μm), SWIR2 (2.0 to 2.5 μm), MIR (3.0 to 5.0 μm), and TIR (8.0 to 12.0 μm)
AISA (Airborne Imaging Spectrometer)	Spectral Imaging www.specim.fi	up to 288	0.43 to 1.0 μm

Table 2. Proposed Space-Based Hyperspectral Sensors

Satellite	Sensor	Sponsoring Agencies
ARIES-I	ARIES-I	Auspace Ltd ACRES Earth Resource Mapping Pty. Ltd. Geoimage Pty. Ltd. CSIRO
PROBA	CHRIS	European Space Agency
NEMO	COIS	Space Technology Development Corporation Naval Research Laboratory
PRISM		European Space Agency

Application of Hyperspectral Image Analysis

Hyperspectral imagery has been used to detect and map a wide variety of materials having characteristic reflectance spectra. For example, hyperspectral images have been used by geologists for mineral mapping (Clark et al., 1992, 1995) and to detect soil properties including moisture, organic content, and salinity (Ben-Dor, 2000). Vegetation scientists have successfully used hyperspectral imagery to identify vegetation species (Clark et al., 1995), study plant canopy chemistry (Aber and Martin, 1995), and detect vegetation stress (Merton, 1999). Military personnel have used hyperspectral imagery to detect military vehicles under partial vegetation canopy, and many other military target detection objectives.

Atmospheric Correction

When sunlight travels from the sun to the Earth's surface and then to the sensor, the intervening atmosphere often scatters some light. Therefore, the light received at the sensor may be more or less than that due to reflectance from the surface alone.

Atmospheric correction attempts to minimize these effects on image spectra.

Atmospheric correction is traditionally considered to be indispensable before quantitative image analysis or change detection using multispectral or hyperspectral data.

Sophisticated atmospheric correction algorithms have been developed to calculate concentrations of atmospheric gases directly from the detailed spectral information contained in hyperspectral imagery, without additional data about atmospheric conditions. Two such algorithms, ACORN from [Analytical Imaging and Geophysics](#) and FLAASH from [Research Systems](#), are available as plug-in modules to ENVI.

Spectral Libraries

Spectral libraries are collections of reflectance spectra measured from materials of known composition, usually in the field or laboratory. Many investigators collect spectral libraries for materials in their field sites as part of every project, to facilitate analysis of multispectral or hyperspectral imagery from those sites. Several high quality spectral libraries are also publicly available (e.g., Clark et al., 1993; Grove et al., 1992; Elvidge, 1990; Korb et al., 1996; Salisbury et al., 1991a; Salisbury et al., 1991b; Salisbury et al., 1994). An ENVI installation includes 27 spectral libraries for a wide variety of materials ranging from minerals and vegetation to manmade materials. Spectra from libraries can guide spectral classifications or define targets to use in spectral image analysis.

Classification and Target Identification in ENVI

There are many unique image analysis algorithms that have been developed to exploit the extensive information contained in hyperspectral imagery. Most of these algorithms also provide accurate, although more limited, analyses of multispectral data. Spectral analysis methods usually compare pixel spectra with a reference spectrum (often called a *target*).

Target spectra can be derived from a variety of sources, including spectral libraries, regions of interest within a spectral image, or individual pixels within a spectral image.

The most commonly used hyperspectral/multispectral image analysis methods that are provided by ENVI are described below.

Whole Pixel Methods

Whole pixel analysis methods attempt to determine whether one or more target materials are abundant within each pixel in a multispectral or hyperspectral image on the basis of the spectral similarity between the pixel and target spectra. Whole-pixel scale tools include standard supervised classifiers such as Minimum Distance or Maximum Likelihood (Richards and Jia, 1999), as well as tools developed specifically for hyperspectral imagery such as Spectral Angle Mapper and Spectral Feature Fitting.

Spectral Angle Mapper (SAM)

Consider a scatter plot of pixel values from two bands of a spectral image. In such a plot, pixel spectra and target spectra will plot as points (Fig. 6). If a vector is drawn from the origin through each point, the angle between any two vectors constitutes the spectral angle between those two points. The Spectral Angle Mapper (Yuhas et al., 1992) computes a spectral angle between each pixel spectrum and each target spectrum. The smaller the spectral angle, the more similar the pixel and target spectra. This spectral angle will be relatively insensitive to changes in pixel illumination because increasing or decreasing illumination doesn't change the direction of the vector, only its magnitude (i.e., a darker pixel will plot along the same vector, but closer to the origin). Note that although this discussion describes the calculated spectral angle using a two-dimensional scatter plot, the actual spectral angle calculation is based on all of the bands in the image. In the case of a hyperspectral image, a spectral "hyper-angle" is calculated between each pixel and each target.

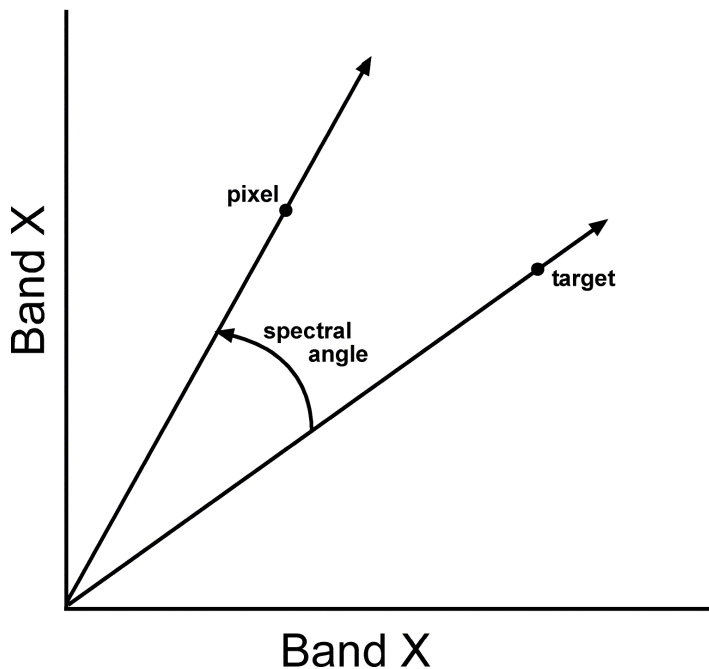


Figure 6. The Spectral Angle Mapper concept.

Spectral Feature Fitting

Another approach to matching target and pixel spectra is by examining specific absorption features in the spectra (Clark et al., 1991). An advanced example of this method, called Tetracorder, has been developed by the U.S. Geological Survey (Clark et

al., 2000). A relatively simple form of this method, called Spectral Feature Fitting, is available as part of ENVI. In Spectral Feature Fitting the user specifies a range of wavelengths within which a unique absorption feature exists for the chosen target. The pixel spectra are then compared to the target spectrum using two measurements: 1) the depth of the feature in the pixel is compared to the depth of the feature in the target, and 2) the shape of the feature in the pixel is compared to the shape of the feature in the target (using a least-squares technique).

Sub-Pixel Methods

Sub-pixel analysis methods can be used to calculate the quantity of target materials in each pixel of an image. Sub-pixel analysis can detect quantities of a target that are much smaller than the pixel size itself. In cases of good spectral contrast between a target and its background, sub-pixel analysis has detected targets covering as little as 1-3% of the pixel. Sub-pixel analysis methods include Complete Linear Spectral Unmixing, and Matched Filtering.

Complete Linear Spectral Unmixing

The set of spectrally unique surface materials existing within a scene are often referred to as the spectral *endmembers* for that scene. Linear Spectral Unmixing (Adams et al., 1986; Boardman, 1989) exploits the theory that the reflectance spectrum of any pixel is the result of linear combinations of the spectra of all endmembers inside that pixel. A linear combination in this context can be thought of as a weighted average, where each endmember weight is directly proportional to the area the pixel containing that endmember. If the spectra of all endmembers in the scene are known, then their abundances within each pixel can be calculated from each pixel's spectrum.

Unmixing simply solves a set of n linear equations for each pixel, where n is the number of bands in the image. The unknown variables in these equations are the fractions of each endmember in the pixel. To be able to solve the linear equations for the unknown pixel fractions it is necessary to have more equations than unknowns, which means that we need more bands than endmember materials. With hyperspectral data this is almost always true.

The results of Linear Spectral Unmixing include one abundance image for each endmember. The pixel values in these images indicate the percentage of the pixel made up of that endmember. For example, if a pixel in an abundance image for the endmember quartz has a value of 0.90, then 90% of the area of the pixel contains quartz. An error image is also usually calculated to help evaluate the success of the unmixing analysis.

Matched Filtering

Matched Filtering (Boardman et al., 1995) is a type of unmixing in which only user-chosen targets are mapped. Unlike Complete Unmixing, we don't need to find the spectra of all endmembers in the scene to get an accurate analysis (hence, this type of analysis is often called a 'partial unmixing' because the unmixing equations are only partially solved). Matched Filtering was originally developed to compute abundances of targets that are relatively rare in the scene. If the target is not rare, special care must be taken when applying and interpreting Matched Filtering results.

Matched Filtering “filters” the input image for good matches to the chosen target spectrum by maximizing the response of the target spectrum within the data and suppressing the response of everything else (which is treated as a composite unknown background to the target). Like Complete Unmixing, a pixel value in the output image is proportional to the fraction of the pixel that contains the target material. Any pixel with a value of 0 or less would be interpreted as background (i.e., none of the target is present).

One potential problem with Matched Filtering is that it is possible to end up with false positive results. One solution to this problem that is available in ENVI is to calculate an additional measure called “infeasibility”. Infeasibility is based on both noise and image statistics and indicates the degree to which the Matched Filtering result is a feasible mixture of the target and the background. Pixels with high infeasibilities are likely to be false positives regardless of their matched filter value.

Summary

Hyperspectral sensors and analyses have provided more information from remotely sensed imagery than ever possible before. As new sensors provide more hyperspectral imagery and new image processing algorithms continue to be developed, hyperspectral imagery is positioned to become one of the most common research, exploration, and monitoring technologies used in a wide variety of fields.

References

- Aber, J. D., and Martin, M. E., 1995, High spectral resolution remote sensing of canopy chemistry. In *Summaries of the Fifth JPL Airborne Earth Science Workshop*, JPL Publication 95-1, v. 1, pp. 1-4.
- Adams, J. B., Smith, M. O., and Johnson, P.E., 1986, Spectral mixture modeling: A new analysis of rock and soil types at the Viking Lander 1 site. *Journal of Geophysical Research*, vol. 91(B8), pp. 8090-8112.
- Ben-Dor, E., Patin, K., Banin, A. and Karnieli, A., 2001, Mapping of several soil properties using DAIS-7915 hyperspectral scanner data. A case study over clayey soils in Israel. *International Journal of Remote Sensing* (in press).
- Boardman, J. W., 1989, Inversion of imaging spectrometry data using singular value decomposition. *Proceedings of the Twelfth Canadian Symposium on Remote Sensing*, v. 4., pp. 2069-2072.
- Boardman, J. W., Kruse, F. A., and Green, R. O., 1995, Mapping target signatures via partial unmixing of AVIRIS data. In *Summaries of the Fifth JPL Airborne Earth Science Workshop*, JPL Publication 95-1, v. 1, pp. 23-26.
- Clark, R. N., and Swayze, G. A., 1995, Mapping minerals, amorphous materials, environmental materials, vegetation, water, ice, and snow, and other materials: The USGS Tricorder Algorithm. In *Summaries of the Fifth Annual JPL Airborne Earth Science Workshop*, JPL Publication 95-1, v. 1, pp. 39 - 40.
- Clark, R. N., Swayze, G. A., Gallagher, A., Gorelick, N., and Kruse, F. A., 1991, Mapping with imaging spectrometer data using the complete band shape least-squares algorithm simultaneously fit to multiple spectral features from multiple

- materials. In Proceedings of the Third Airborne Visible/Infrared Imaging Spectrometer (AVIRIS) workshop, JPL Publication 91-28, pp. 2-3.
- Clark, R. N., Swayze, G. A., and Gallagher, A., 1992, Mapping the mineralogy and lithology of Canyonlands, Utah with imaging spectrometer data and the multiple spectral feature mapping algorithm. In Summaries of the Third Annual JPL Airborne Geoscience Workshop, JPL Publication 92-14, v 1, pp. 11-13.
- Clark, R. N., Swayze, G. A., Gallagher, A. J., King, T. V. V., and Calvin, W. M., 1993, The U. S. Geological Survey, Digital Spectral Library. Version 1: 0.2 to 3.0 microns. U.S. Geological Survey Open File Report 93-592, 1340 pages.
- Clark, R. N., Swayze, G. A., King, T. V. V., 2001, Imaging Spectroscopy: A Tool for Earth and Planetary System Science Remote Sensing with the USGS Tetracorder Algorithm, *Journal of Geophysical Research* (submitted).
- Elvidge, C. D., 1990, Visible and infrared reflectance characteristics of dry plant materials. *International Journal of Remote Sensing*, v. 11(10), pp. 1775 - 1795.
- Grove, C. I., Hook, S. J., and Paylor, E. D., 1992, Laboratory reflectance spectra for 160 minerals 0.4 - 2.5 micrometers. JPL Publication 92-2.
- King, R. N., Trude, V. V., Ager, C., and Swayze, G. A., 1995, Initial vegetation species and senescence/stress indicator mapping in the San Luis Valley, Colorado using imaging spectrometer data. In Summaries of The Fifth Annual JPL Airborne Earth Science Workshop, vol. 1, p. 35-38.
- Korb, A. R., Dybwad, P., Wadsworth, W., and Salisbury, J. W., 1996, Portable FTIR spectrometer for field measurements of radiance and emissivity. *Applied Optics*, v. 35, pp. 1679-1692.
- Merton, R. N., 1999, Multi-temporal analysis of community scale vegetation stress with imaging spectroscopy. Ph.D. Thesis, Geography Department, University of Auckland, New Zealand, 492p.
- Richards, J.A., and Jia, X., 1999, *Remote Sensing Digital Image Analysis, an Introduction*. Third Edition. Springer-Verlag: Berlin.
- Salisbury, J. W., D'Aria, D. M., and Jarosevich, E., 1991a, Midinfrared (2.5-13.5 micrometers) reflectance spectra of powdered stony meteorites. *Icarus*, v. 92, pp. 280-297.
- Salisbury, J. W., Wald, A., and D'Aria, D. M., 1994, Thermal-infrared remote sensing and Kirchhoff's law 1. Laboratory measurements. *Journal of Geophysical Research*, v. 99, pp. 11,897-11,911.
- Salisbury, J. W., Walter, L. S., Vergo, N., and D'Aria, D. M., 1991b, Infrared (2.1- 25 micrometers) Spectra of Minerals. Johns Hopkins University Press, 294 p.
- Yuhas, R.H., Goetz, A. F. H., and Boardman, J. W., 1992, Discrimination among semi-arid landscape endmembers using the spectral angle mapper (SAM) algorithm. In Summaries of the Third Annual JPL Airborne Geoscience Workshop, JPL Publication 92-14, vol. 1, pp. 147-149.

Author

Peg Shippert is the Earth Science Applications Specialist for Research Systems, Inc. (www.researchsystems.com), the makers of ENVI and IDL and a wholly owned subsidiary of Eastman Kodak. She has a Ph.D. in physical geography and more than 13 years of experience analyzing multispectral and hyperspectral imagery for a wide variety of applications.